Temporal Variations In Vapor Intrusion-Induced Indoor Air Contaminant Concentrations

Jonathan G. V. Ström, Yijun Yao, and Eric M. Suuberg*

Brown University, School of Engineering, Providence, RI, USA

E-mail: eric_suuberg@brown.edu

Abstract

Introduction

Long term vapor intrusion (VI) studies in both residential and larger commercial structures have raised concerns regarding significant observed transient behavior in indoor air contaminant concentrations.[1–7] Such variations make it difficult for those charged with protecting human health to formulate a response should evaluation of the risk of exposure be based upon observed peak concentrations, or long-term averages, or something else? There is even uncertainty within the VI community regarding how to best develop sampling strategies to address this problem.[1,3,8] What represents a reasonable sampling strategy for a particular site a single 8 hr sample? Repeated 8 hr samples? Month-long samples? Continuous monitoring?

VI involves the migration of volatilizing contaminants from soil, groundwater or other subsurface sources into overlying structures. The basic nature of VI has been understood for some time and it has been the subject of much study, but some aspects remain poorly

understood, such as the causes of the sometimes observed large temporal transients in indoor air concentrations. Results from a house operated by Arizona State University (ASU) near Hill AFB in Utah, an EPA experimental house in Indianapolis, IN and a large warehouse at the Naval Air Station (NAS) North Island, CA have all shown significant transient variations in indoor air contaminant concentrations. All were outfitted with sampling and monitoring equipment that allowed tracking temporal variation in indoor air contaminant concentrations on time scales of hours. All have shown that these concentrations vary significantly with time - orders of magnitude on the timescale of a day or days.[5,9,10]

In one instance the source of the variation was clearly established during the study of the site. At the ASU house a drain pipe (or "land drain") connected to a sewer system was discovered beneath the house. Careful isolation of this source led to a clear conclusion that this "preferential pathway" for contaminant vapor migration significantly contributed to observed indoor air contaminant levels and their fluctuations.[10,11] While in this case the issue of a contribution from a preferential pathway was clearly resolved, what it left open was a question of whether existence of such a preferential pathway would always be expected to lead to large fluctuations in indoor air contaminant concentrations.

Similarly, a sewer pipe has recently been suggested to be a source of the contaminants found in the EPA Indianapolis house. That site was also characterized by large indoor air contaminant concentration fluctuations.[7,12] Sewer lines have been previously implicated as VI sources at several sites.[12–15] A Danish study has estimated that roughly 20% of all VI sites in central Denmark involve significant sewer VI pathways.[16] Thus while consideration of sewer or other preferential pathways is now part of normal good practice in VI site investigation,[1] it is still not known whether the existence of such pathways automatically means that large temporal fluctuations are necessarily to be expected.

In some of the above cited cases,[13,15] a sewer provided a pathway for direct entry of contaminant into the living space. While potentially important in many instances, this scenario is not further considered here where the focus is on pathways that deliver contaminant via

the soil beneath a structure. It is, however, now known that even absent a preferential pathway, there may be significant transient variation in indoor air contaminant concentrations at VI sites.[2,4,17] One example is the site at NAS North Island at which no preferential pathways have been identified. Instead, a building at this site is characterized by significant temporal variations in indoor-outdoor pressure differential.[5] It is believed that this is the origin of the observed indoor air contaminant concentration fluctuations at that site.

This paper investigates the sources of the temporal variation in indoor air contaminant concentrations in both the presence and absence of preferential pathways. In this work, the latter scenarios are referred to as "normal" VI scenarios, in which there is typically a groundwater source of the contaminant. Specifically, we pose the question of just how much variation in indoor air contaminant concentration may be expected at such normal VI sites vs. those characterized by preferential pathways within the soil beneath the site. The conditions required for preferential pathways to become significant contributors to temporal variations in indoor air contaminant concentrations are also explored, and the consequences for sampling strategies are discussed.

Methods

Statistical Analysis Of Field Data

To frame the question of just how much variability in indoor air contaminant concentrations is actually seen, field datasets have been analyzed. For this purpose, datasets from the ASU house in Utah, the EPA Indianapolis site and North Island NAS were chosen for analysis. Readers are referred to the original published works for details regarding data acquisition.[3,5,7,9,10]

The ASU house data were obtained over a period of several years. During part of this time, controlled pressure method (CPM) tests were being conducted, in which the house was underpressurized to an extent greater than that characterizing "normal" house operation thus

Figure 1: Typical data on indoor air TCE contaminant concentrations at the Indianapolis site.[7]

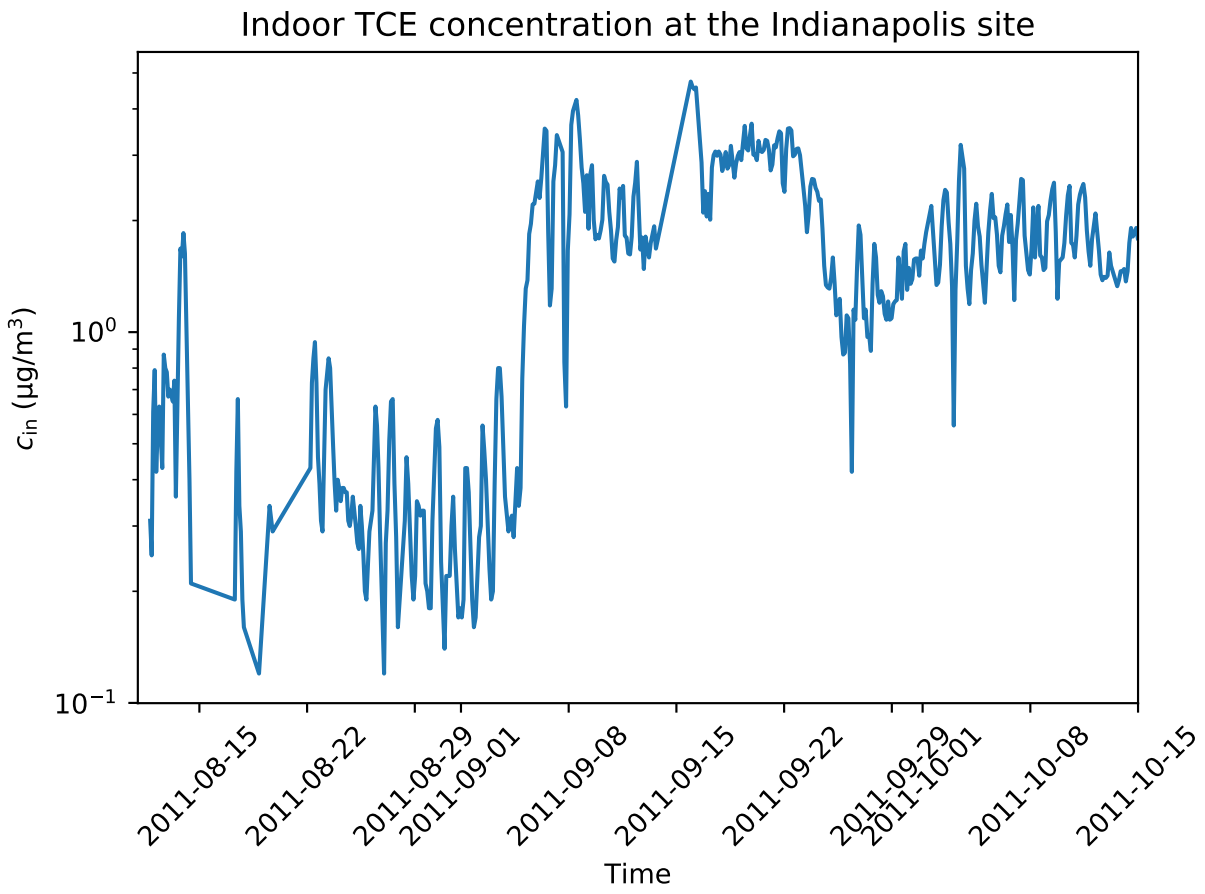

increasing VI potential.[6,9,18] The period of CPM testing is thus excluded from the analysis. Likewise, the existence of a preferential pathway at the ASU house needs to be considered in examining that dataset; during some of the testing at that site, this pathway was cut off, resulting in "normal" VI conditions in which the main source of contaminant was diffusion of contaminant vapor from an underlying groundwater source.

The NAS North Island dataset has not (as far as is known) been influenced by a preferential pathway, but the structure there was subject to "large" internal pressure fluctuations. By "large" is meant still only of order 10-20 Pa, but these were greater than those generally recorded at the ASU house during normal operations. The underlying soil at NAS North Island is sandy[5] and more permeable than that at the ASU site, which will be shown to lead to greater pressure sensitivity in the former case.

The Indianapolis site investigation also spanned a number of years and periodically included the testing of a sub-slab depressurziation system (SSD) for VI mitigation. Only the period before the installation of this system was considered in the present analysis. It is likely a sewer line beneath the structure acted as a preferential pathway.[12] Unlike at the ASU house, this preferential pathway was never removed or blocked, making it impossible to isolate the role of the preferential pathway at this site. It is still of interest to consider the data from this site because of the completeness and extensiveness of the data collection. Figure 1 illustrates a typical reported series of indoor air trichloroethylene (TCE) concentration measurements from this site. There is almost a two order of magnitude variation in the concentration data.

Some of the analysis of the above three field data sets relies on a probability density estimation technique called "kernel density estimation" (KDE). KDE is a technique used for estimating the probability distribution of a random variable(s) by using multiple kernels, or weighting functions to characterize the data sets. In this case, Gaussian kernels are used to create the KDEs. This means that it is presumed that the variables of interest (i.e., indoor air contaminant concentrations and indoor-outdoor pressure differentials, as sampled) are

normally distributed around mean values and that there are statistical fluctuations associated with each sampling event. In this instance, the scipy statistical package was used to construct the KDEs, assuming a bandwidth parameter determined by Scott's rue. The SciPy Python library was used to conduct all statistical analysis and data processing.[19]

Modeling Work

Figure 2: Foundation and vadose zone soil represented in the modeling. Note that here a gravel sub-base material is shown, but in certain simulations, that material is absent and the surrounding soil directly contacts the foundation slab. Different assumptions are made regarding the preferential pathway, here shown as a pipe entering the gravel sub-base. In some cases, the preferential pathway has been "turned off".

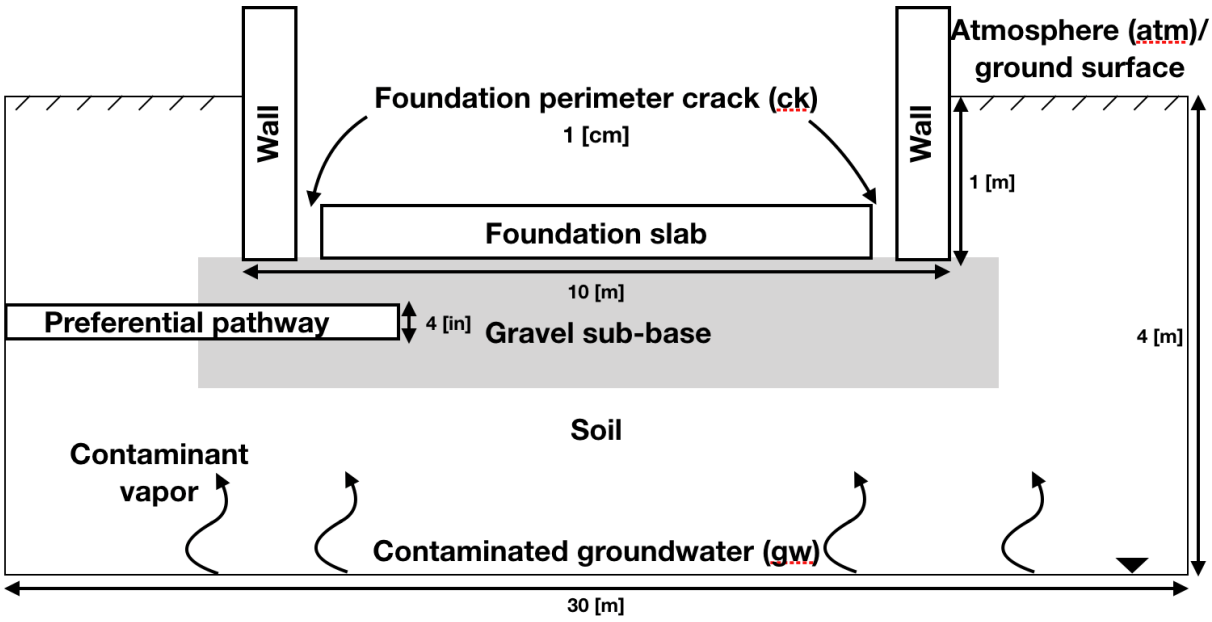

A previously described three-dimensional computational fluid dynamics model of a generic VI impacted house has been used to elucidate certain aspects of transient VI processes. In the present work, there has been an addition of a preferential pathway to the "standard" model that has been described before in publications by this group.[20–22] As in the earlier studies, only the vadose zone soil domain is directly modeled. Figure 2 shows a cutaway view of the relevant modeling domain.

The modeled VI impacted structure is assumed to have a 10x10 m foundation footprint, with the bottom of the foundation slab lying 1 m below ground surface (bgs), simulating a house with a basement. The indoor air space is modeled as a continuously stirred tank (CST)[1] and all of the contaminant entering the house is assumed to enter with soil gas through a 1 cm wide crack located between the foundation walls and the foundation slab around the perimeter of the house. All of the contaminant leaving the indoor air space is assumed to do so via air exchange with the ambient. The indoor control volume is here assumed to consist of only of the basement, having a total volume of 300 m^3. Clearly different assumptions could be made regarding the structural features and the size of the crack entry route, but for present purposes, this is unimportant as the intent is only to show for "typical" values what the influence of some critical parameters is.

The modeled surrounding soil domain extends 5 meters from the perimeter of the house and is assumed to consist of sandy loam, except as noted otherwise. Directly beneath the foundation slab, there is assumed to be a 30 cm (one foot) thick gravel layer, except in certain cases here this sub-base material is assumed to be the same as the surrounding soil (termed a "uniform" soil scenario). The groundwater beneath the structure is assumed to be homogeneously contaminated with TCE selected as a prototypical contaminant. The groundwater itself is not modeled, as the bottom of the model domain is defined by the top of the water table. Where relevant, the preferential pathway is modeled as a 10 cm (4") pipe that opens into the gravel sub-base beneath the structure. The air in the pipe is also assumed to be contaminated with TCE at a vapor concentration equal to the vapor in equilibrium with the groundwater contaminant concentration below the structure, modified by a scaling factor χ (allowing the contaminant concentration in the pipe to be parameterized). This model illustrates the concept of a "preferential pathway", as the pipe carries contaminant vapor to the immediate vicinity of the foundation, by a path that circumvents the usual soil diffusion pathway.

The ground surface and the pipe are both sources of air to the soil domain. Both are

assumed to exist be at reference atmospheric pressure. Soil gas transport is governed by Richard's equation, a modified version of Darcy's Law, taking the variability of soil moisture in the vadose zone into account.[23] The van Genuchten equations are used to predict the soil moisture content and thus the effective permeability of the soil.[24] The effective diffusivity of contaminant in soil is calculated using the Millington-Quirk model.[25] The transport of contaminant vapor in the soil is assumed to be governed by the advection-diffusion equation, in which either advection or diffusion may dominate depending upon position and particular circumstances. The key working equations and the boundary conditions are summarized in Table 1.

Results & Discussion

Variation In Indoor Air Contaminant Concentration Over Time

High frequency measurement of indoor air contaminant concentrations, c_{in} , such as those in Figure 1, took place at both the ASU House and the Indianapolis House over significant periods.[3,7] Furthermore, at the Indianapolis site the c_{in} for three different contaminants, chloroform, TCE, and tetrachloroethylene (PCE) were all collected, allowing examination of the variability of each VI contaminant. The NAS North Island NAS dataset was obtained over a much shorter duration, and is therefore not examined in this portion of the analysis.

Figure 1 showed a large degree of temporal variation in one of the components, and the data for the other components were quite similar. What is apparent upon closer examination of such data is that the actual day-to-day variations are typically not nearly as large as those observed when tracking the data for a longer time. To demonstrate this point, the quotient of the maximum and minimum c_{in} values (denoted as $c_{\max}/c_{\min}$) are shown as a function of time in Figure 3. The values shown in Figure 3 are the means of the quotients calculated for samples separated by the indicated times and the error bars indicate the 95th percentile of all the data points. Hypothetical resampling periods of one, two, three days, and the same

Table 1: Governing equations, boundary conditions & model input parameters. (See below for table of nomenclature).

(a) Governing equations

Unsteady-CST	$V\frac{dc_{\text{in}}}{dt} = \int_{A_{\text{ck}}} j_{\text{ck}} dA - c_{\text{in}} A_e V_{\text{slab}}$
Richard's equation	$\nabla \cdot \rho\Big(-\frac{\kappa_s}{\mu} k_r \nabla p\Big) = 0$
Millington-Quirk	$D_{\text{eff}} = D_{\text{air}} \frac{\theta_g^{10/3}}{\theta_t^2} + \frac{D_{\text{water}}}{K_H} \frac{\theta_w^{10/3}}{\theta_t^2}$
Advection-diffusion equation	$\frac{\partial}{\partial t}\Big(\theta_w c_w + \theta_g c\Big) = \nabla(D_{\text{eff}} \cdot \nabla c) - \vec{u} \cdot \nabla c$
van Genuchten equations	$\text{Se} = \frac{\theta_w - \theta_r}{\theta_t - \theta_r} = [1 + \lvert\alpha z\rvert^n]^{-m}$ $\theta_g = \theta_t - \theta_w$ $k_r = (1 - \text{Se})^l [1 - (\text{Se}^{-m})^m]^2$ $m = 1 - 1/n$

(b) Boundary conditions

Boundary	**Richard's equation**	**Advection-diffusion equation**
Foundation crack	$p = p_{\text{in/out}}$ (Pa)	$j_{\text{ck}} = \frac{uc}{1 - \exp(uL_{\text{slab}}/D_{\text{air}})}$
Groundwater source	*No flow*	$c = c_{\text{gw}} K_H$ (μg/m^3)
Groundsurface	$p = 0$ (Pa)	$c = 0$ (μg/m^3)
Preferential pathway	$p = 0$ (Pa)	$c = c_{\text{gw}} K_H \chi$ (μg/m^3)

(c) Soil & gravel properties[26–28]

Soil	κ_s (m^2)	ρ (kg/m^3)	θ_s	θ_r	α (1/m)	n
Gravel	$1.3 \cdot 10^{-9}$	1680	0.42	0.005	100	3.1
Sandy Loam	$5.9 \cdot 10^{-13}$	1460	0.39	0.039	2.7	1.4

(d) Trichloroethylene (diluted in air) properties[27,28]

D_{air} (m^2/h)	D_{water} (m^2/h)	ρ (kg/m^3)	μ (Pa $\cdot$ s)	K_H	M (g/mol)
$2.47 \cdot 10^{-2}$	$3.67 \cdot 10^{-6}$	1.614	$1.86 \cdot 10^{-5}$	0.403	131.39

(e) Building properties

V_{base} (m^3)	L_{slab} (cm)	A_e (1/hr)
300	15	0.5

number of weeks, and months were chosen.

For example, if the data are examined in terms of the mean maximum variation observable over the course of 24 hours (one day) the variation is no greater than about a factor of two

Figure 3: Mean values of the maximum change in indoor air contaminant concentration that may be expected over a given time period. (e.g., 1D is 1 day, 2W is 2 weeks, and 3M is 3 months). The error bars are the 95% confidence intervals.

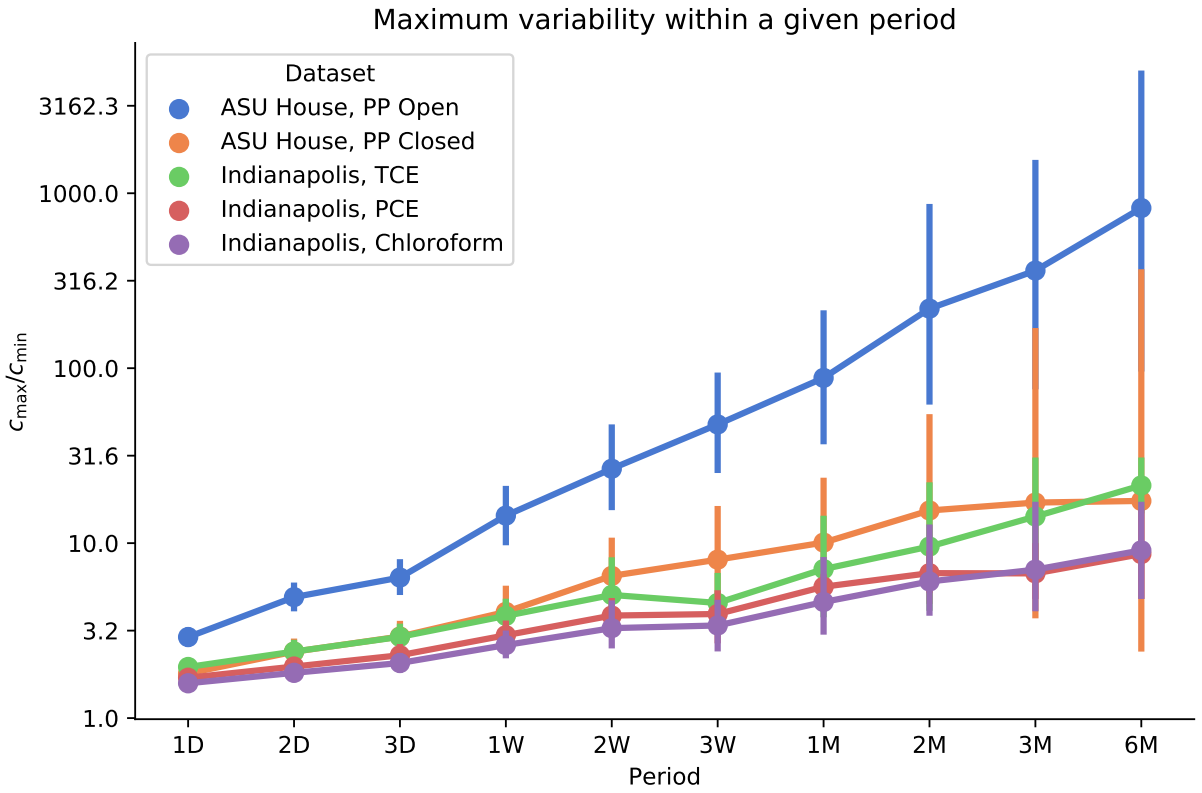

for any of the contaminants at the Indianapolis house or for TCE at the ASU house (when the preferential pathway was closed). The mean variability at the latter was only a bit higher (about a factor of 3) when the preferential pathway was open. In other words, a sampling protocol that involves sampling on two consecutive days would typically not uncover the large temporal variations that characterize the site over longer periods of time. As Figure 1 shows, there are certainly isolated days in which a larger daily change was observed, but these were not typical, to the extent that they fall outside of the 95% criteria used in defining the error bars. So while such unusual jumps might be seen (for unknown reasons) in a very small percentage of cases, the expectation is much more represented by what is shown in Figure 3.

Weeks of temporal separation in sampling events are required to observe the large vari-

ations of concern. Orders of magnitude differences begin to manifest themselves over the course of months. This is not surprising, since those who performed the measurements have already reported that there were seasonal aspects to the values obtained. This would be consistent with requiring months to see the more significant variations.

This analysis also suggests that certain types of preferential pathways contribute to larger variations on shorter timescales (ASU House). Even though there was a preferential pathway present at the Indianapolis House, the transients associated with its presence were of a slower nature and the behavior was not unlike what was observed at ASU House when the preferential pathway was closed. This warns that the mere existence of a preferential pathway is not by itself sufficient to create a situation of large variations over short sampling times.

The longer the resampling period, the larger the maximum variability in observed indoor air contaminant concentrations. In the case of the ASU House with the preferential pathway open, the variability went from less than a threefold difference on the timescale of a day, to two to three orders of magnitude over the course of weeks. Thus there are different timescales that characterize different extents of variation, again pointing to the existence of more than a single factor that determines variability.

If the maximum observed variability is quite small across only a few days as these data suggest, a sampling strategy that involves taking daily samples for several days in a row will likely yield little extra useful information beyond what can be obtained with a single sample.

Statistical Analysis of Field Data

Table 2: 5th and 95th percentile values of $p_{\text{in/out}}$ and $c_{\text{in}}/c_{\text{in,mean}}$ in Figure 4.

	North Island NAS		**ASU house PP Open**		**ASU House PP Closed**	
Percentile	5th	95th	5th	95th	5th	95th
$p_{\text{in/out}}$ (Pa)	-19.9	7.4	-1.4	2.1	-2.1	2.27
$c_{\text{in}}/c_{\text{in,mean}}$	4.1	0.2	13.5	0.2	3.3	0.4

Figure 4: 2D-KDE plot showing the distributions of indoor air contaminant concentration, the indoor/outdoor pressure difference, and how they correlate to each other.

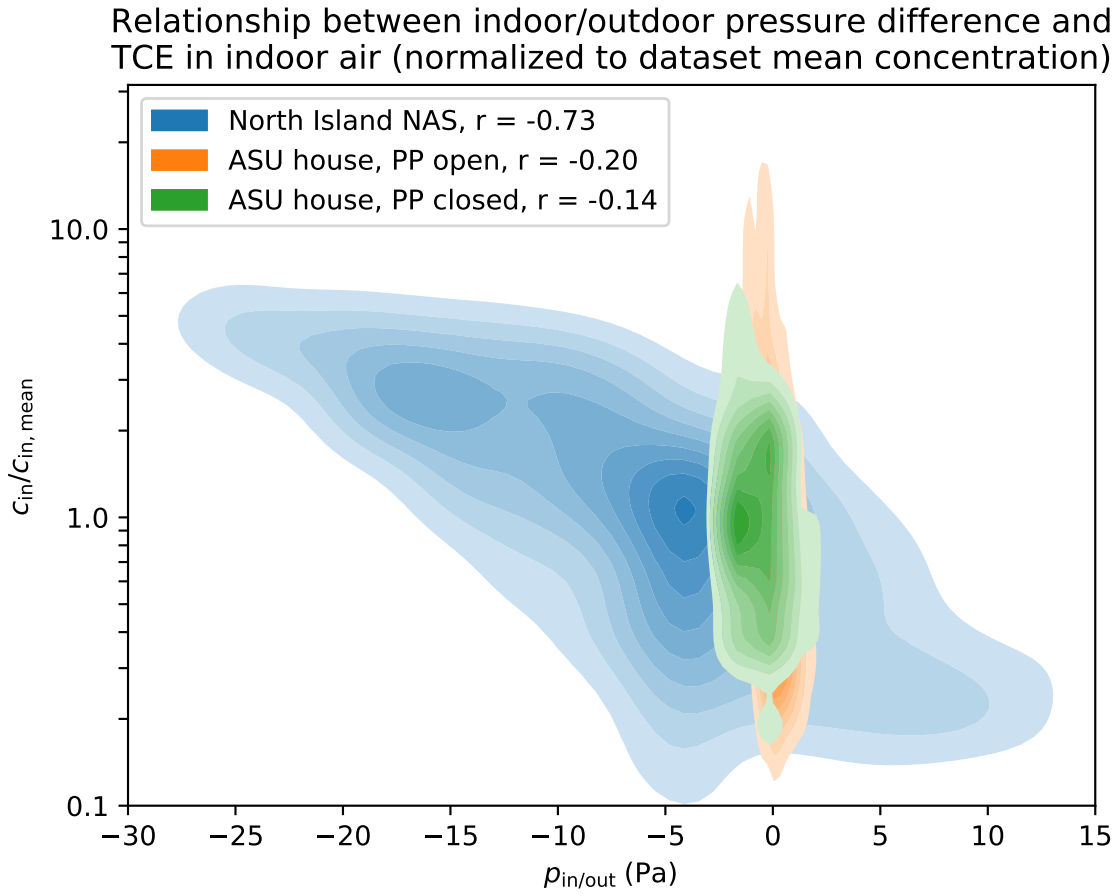

The data in Figure 1 and Figure 3 raise the question of what then actually determines the large degree of temporal variation sometimes reported. The rate of advective entry of soil gas into a structure is frequently cited as playing an important role in determining entry rate of contaminant. This advective entry rate is closely linked to the indoor-outdoor pressure difference, as can be caused by the "stack effect", for example. Thus we first consider how much variability there might be in the pressure driving force for advection, and if this can explain the observed variability in observed indoor air contaminant concentrations.

The pressure difference between the indoor and outdoor/ambient ($p_{\mathrm{in/out}}$) leads to advection, by which contaminants are drawn into (or prevented from) entering a structure. Changes in $p_{\mathrm{in/out}}$ can take place quickly, leaving open the possibility of their impacting VI far more

rapidly than can fluctuations in say groundwater depth or contaminant concentration (these latter processes take weeks or even months to impact the overlying structure).

We examine the relationship between $p_{\text{in/out}}$ and c_{in} by constructing the two-dimensional kernel density estimation (KDE) plots seen in Figure 4. The KDE plots allow us to view the measured distributions of $p_{\text{in/out}}$ and c_{in}, and develop a visual impression of how well these distributions correlate with one another. For this analysis we considered two VI sites, NAS North Island and the ASU House. The ASU House dataset was divided into two periods, one before and the other after the land drain (called the preferential pathway (PP) from ere on) had been closed. By comparing these two periods on a single plot, the impact of the preferential pathway becomes clearer.

In Figure 4, the indoor air contaminant concentration c_{in} is normalized to the mean $c_{\text{in,mean}}$ of each dataset, allowing comparison of the impact $p_{\text{in/out}}$ on c_{in} independently from the large differences in absolute values of indoor air concentrations at the different sites. A value of 10 on the y-axis indicates that the corresponding plotted value of c_{in} is 10 times greater than the mean for the dataset, and 0.1 indicate that it is one tenth of the mean.

Inspection of the range of normalized c_{in} values in Figure 4 again shows the two order of magnitude spread in observed values, implying a sampling at one particular time might give a value that is two orders of magnitude different than a result from a different time. Such issues have of course already been pointed out by the investigators who obtained the data.

The power of this KDE representation is that it permits evaluation of the relationship of two independently measured data - the indoor air contaminant concentration and the indoor-outdoor pressure difference. Examining the data in this manner immediately points to an important difference between the data from the ASU House and those from NAS North Island. At NAS North Island site $p_{\text{in/out}}$ varies significantly; the 5th and 95th percentile of $p_{\text{in/out}}$ are -19.9 and 7.4 Pa respectively. This may be contrasted with 5th and 95th percentile $p_{\text{in/out}}$ at the ASU house: -1.4 and 2.1 Pa (with the PP open), and -2.1 and 2.27 Pa (PP closed).

The much larger under- and overpressurization of the NAS North Island site compared to the ASU House makes the pressure dependence of indoor air concentration much more visible at the former site. The Pearson's r-value for the correlation between $p_{\mathrm{in/out}}$ and c_{in} for each dataset is shown in the legend, and confirms what is apparent to the eye; the pressure driving force is a determining factor for observed contamination at NAS North Island. But the broadness of the band of the NAS North Island concentration data set suggests that there is still a source of variability in c_{in} that has not been fully captured - this will be addressed below.

The ASU house datasets offer a different picture. The variability of c_{in} is just as large, or even larger than at NAS North Island, yet the $p_{\mathrm{in/out}}$ varied far less. The weaker dependence of c_{in} on the pressure difference is confirmed by the much lower r-values for the correlations between the variables. In other words, there is not nearly as strong a correlation between variation in indoor air contaminant concentration and pressure difference for the ASU House as there was for NAS North Island.

It should be noted that control of indoor depressurization is the principle that underlies the controlled pressure method (CPM) for assessing the potential severity of a VI situation. These results strongly suggest that there are other factors besides indoor pressure determining indoor air contaminant concentrations, and their variations, that may not be accounted for in applying this method.

The data for the ASU House also offer an insight into the role of the preferential pathway. At first glance it may seem like the c_{in} values for the periods when the PP is open and closed are relatively comparable. However, the 5th and 95th percentiles values of $c_{\mathrm{in}}/c_{\mathrm{in,mean}}$ differ significantly as may be seen in Table 2. It is clear that existence of the preferential pathway dramatically increases the variability in indoor air contaminant concentration. This again is entirely consistent with what the investigators of that site have already reported.[11] The correlation with indoor-outdoor pressure difference is weak in the ASU house cases, so there are clearly factors other than pressure difference that determine the variability in each. These

will be explored with the help of a modeling analysis presented below.

Variability Of Attenuation From Subslab

Figure 5: Boxplot of $\log_{10}$ (subslab to indoor air contaminant attenuation) at the ASU house site. The box shows the quartiles of the distribution, the whiskers the extent of the distribution, and diamonds are points that are considered outliers.

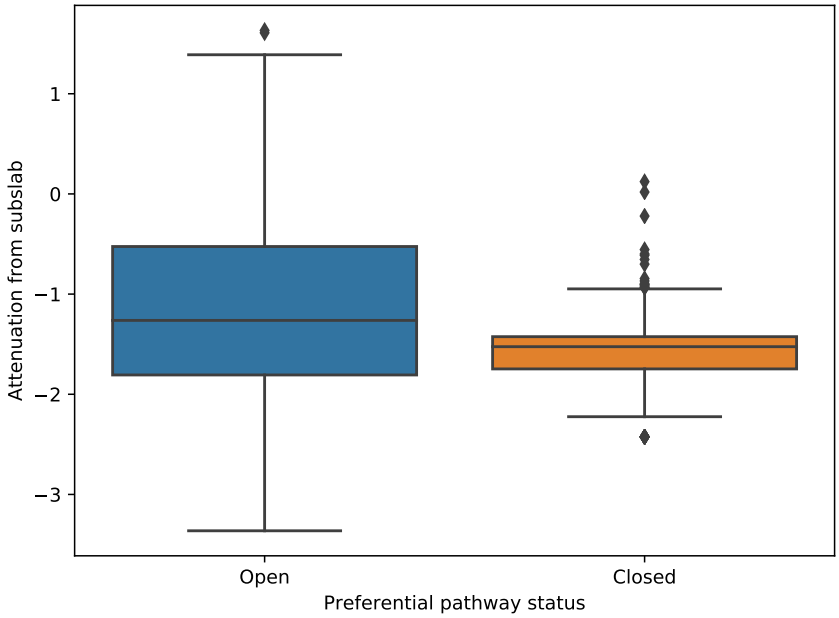

Observed temporal variations in indoor air contaminant concentrations might be explained by temporal variations in subslab contaminant concentrations. To examine how variability in subslab contaminant concentration might contribute to variability in indoor air contaminant concentration, data on the attenuation from subslab ($\alpha_{\text{subslab}} = c_{\text{in}}/c_{\text{subslab}}$) were examined. The dataset utilized for this was that from the ASU House. The c_{subslab} values were taken from a soil gas probe labeled as "6" at the ASU house. This probe was located closest to both the exit of the preferential pathway pipe, and to a reported breach in the foundation that served as a key entry pathway for contaminant getting into the house.[11] The results are shown in Figure 5.

It is apparent that during the period when the preferential pathway was closed, α_{subslab} did not vary significantly, and was quite close to the EPA recommended α_{subslab} value of

0.03.[1] Thus during the period when the preferential pathway was closed large temporal variations in subslab concentrations could not have been driving the variations in indoor air contaminant concentrations.

When the PP was open, there was considerably more variability in the subslab concentration values, and the mean value was higher than in the case where the preferential pathway was closed. It was also not uncommon for the observed α_{subslab} to exceed unity. While large α_{subslab} values may sometimes indicate indoor sources at a site, there were none at the ASU house. A more likely explanation is that even though probe "6" was located in close proximity to the exit of the preferential pathway, there might have still existed significant spatial variability in c_{subslab} that could not be captured with a single measurement. This suggests caution is needed in profiling subslab contaminant concentrations in the presence of preferential pathways - significant variations are possible.

What the results of Figure 5 do clearly show is that the existence of a preferential pathway of the kind at ASU House (and idealized in Figure 1) can influence the temporal variation of subslab concentrations in a much less predictable way than those observed in "normal" VI scenarios.

Modeling Results

Pressure Effects

Having established the potential impacts of certain inputs on determining variability in indoor air contaminant concentrations, the mathematical model of VI can help further elucidate other key aspects. The results of calculations on a scenario corresponding to Figure 2 are presented in Figure 6. This scenario is not intended to exactly represent the situation at ASU House, but it is similar in the key aspect of having a preferential pathway delivering contaminant to a gravel sub-base. The full, complex geometry of the ASU House has not been represented, but the modeled structure is of comparable size, and will be subject to operational parameters based upon what were measured at that site. The general modeling

Figure 6: Simulated preferential pathway scenarios compared to ASU house field data (top panel). No preferential pathway scenarios in bottom panel. Field data is binned in 40 evenly spaced bins, with the dot representing the mean and errors bars represent the 95% confidence interval. Shaded blue represent the predicted variability due to air exchange rate (using 5th and 95th percentile values).

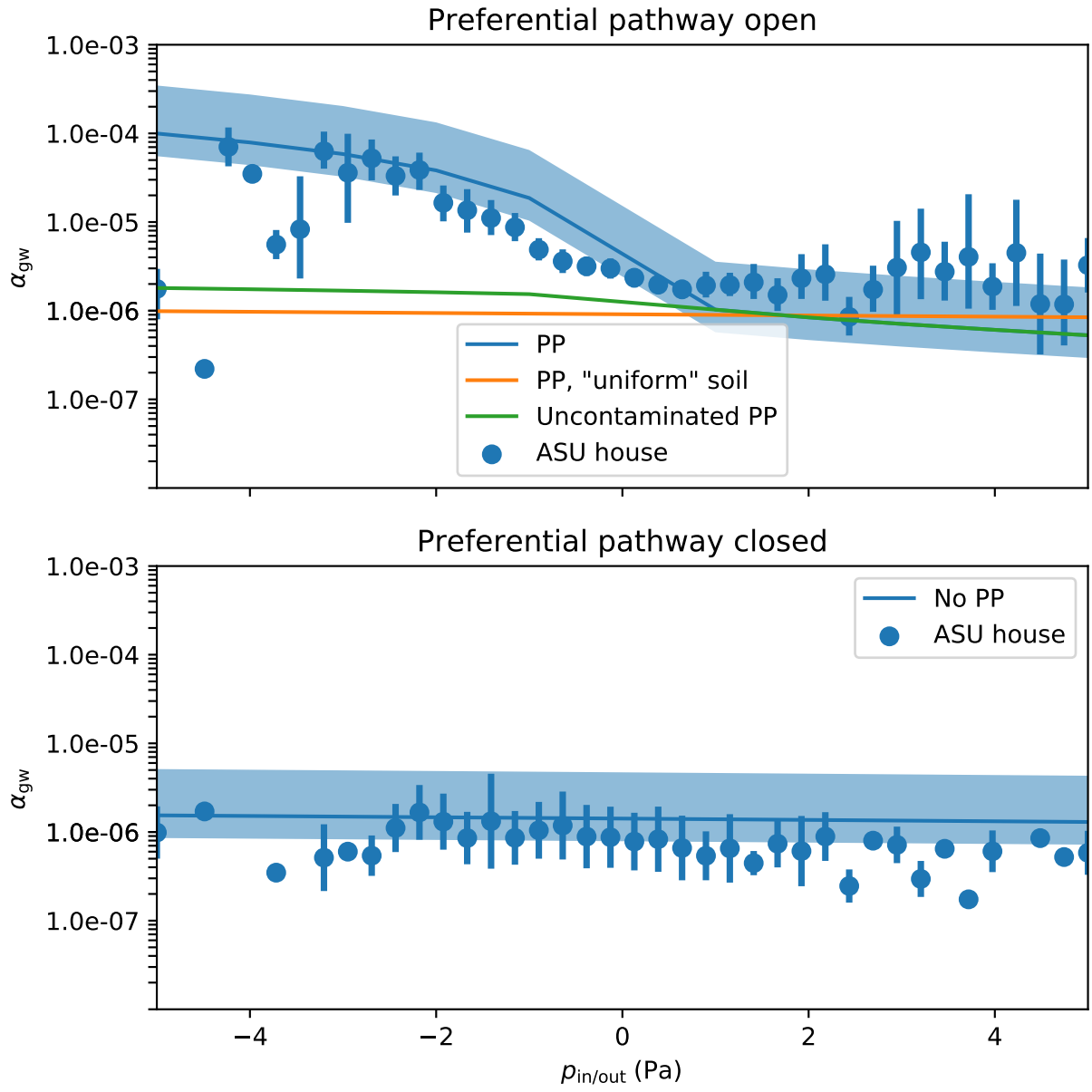

conditions are those shown in Table 1.

In the calculation whose results are shown in the top panel of Figure 6, a preferential pathway is assumed to provide air containing contaminant vapor at a concentration equiva-

lent to the vapor in equilibrium with the underlying groundwater source. Here, the indoor air exchange rate A_e was assumed to be a constant 0.5 per hour, and $p_{\mathrm{in/out}}$ was varied from -5 to 5 Pa. Values of predicted indoor air contaminant concentrations, c_{in} were obtained from steady state calculations. The predicted c_{in} values were then normalized by the assumed vapor concentration in equilibrium with groundwater cgw, giving the attenuation from groundwater α_{gw} . The predicted values of α_{gw} as a function of $p_{\mathrm{in/out}}$ are given by the central blue line in the upper panel of Figure 6. These predicted values are compared to actual measured α_{gw} values from the ASU House for the period during which the preferential pathway was open (blue points).

The model successfully predicts the observed trends in α_{gw} as $p_{\mathrm{in/out}}$ decreases (increased depressurization) but somewhat underpredicts α_{gw} as the house is overpressurized. Most significantly, the model captures that even for a small increase in depressurization (0 to -5 Pa) a very large increase in α_{gw} (two order of magnitude) can occur.

The asymmetry relative to the predictions for depressurization and overpressurization is due to two factors. First, the preferential pathway acts not only as a source of contaminant vapor, but also as a source of air to the subslab. Because of the large resistance to soil gas flow in the surrounding soil, having a local source of air to support the increase of advective flow into the structure from the subslab region makes a large difference.

The above was proven by a second simulation, where the model was rerun with the preferential pathway present, but with the permeable (gravel) layer in the subslab removed and replaced by the surrounding soil (sandy loam). This gave a "uniform soil" scenario the results of which are shown as an orange line in the top panel of Figure 6. This simulation demonstrates that without a permeable subslab to effectively allow the "advective potential" to be realized, existence of preferential pathway way actually not impact a VI site very much. In order for a preferential pathway to significantly contribute to VI, this requires a scenario involving good advective communication between it the indoor environment. These requirements were met at the ASU House.

A perhaps obvious second requirement is that the preferential pathway must deliver contaminant vapors to be impactful. In another simulation, the permeable (gravel) subslab region was included, but the preferential pathway merely delivered clean air to the subslab. The result of this simulation is shown as the green line in the top panel of Figure 6. This shows that while there was a lightly larger $\alpha_{\rm gw}$ compared to the "uniform soil" scenario, it is nowhere near as significant as when the preferential pathway delivers contaminant vapors. The contaminated and uncontaminated preferential pathway scenarios (blue and green lines respectively) thus bound the range of $\alpha_{\rm gw}$ that would be observed for a given $p_{\rm in/out}$ depending on the contaminant vapor concentration in the preferential pathway.

The model is also able to capture the weak trend in $\alpha_{\rm gw}$ with $p_{\rm in/out}$ when a preferential pathway is absent, when there exists a permeable subslab region. These results are shown as the bottom panel in Figure 6. These results are again in agreement with what was observed at the ASU House when the preferential pathway was closed.

What the above simulations fail to predict is the actual observed variability of $\alpha_{\rm gw}$ at any given $p_{\rm in/out}$. This variability is captured by the error bars around the data points in the two panels (denoting one standard deviation). This variability is roughly an order of magnitude. Examining Figure 2 for the case in which the preferential pathway is closed, the "cloud" of data similarly reflect that there is still not captured in the modeling a parameter that determines this variation, independently of the pressure effects.

One other feature of this simulation that warrants noting is that the examined range from $p_{\rm in/out}$ from -5 to +5 Pa is larger than the "usual" range from -2 to +2 Pa observed at the ASU House (as may be seen from Figure 2). The data at larger and smaller values of $p_{\rm in/out}$ were rather sparse, though there were enough points so that the data for the higher range of pressures could be presented in Figure 6. But focusing on the range from -2 to + 2 Pa alone, the pressure dependence of variability is much less visible, just as the data of Figure 2 suggested. This again means that there is a need to explore other reasons for the order of magnitude spread seen in concentration data, when the preferential pathway is closed.

Air Exchange Rate Effects

Table 3: Air exchange rate values (1/hr)

Percentile	**10th**	**50th**	**90th**
EPA[29,30]	0.16-0.2	0.35-0.49	1.21-1.49
ASU house[3,11]	0.21	0.43	0.78
Indianapolis[7]	0.34	0.74	1.27

Table 3 shows the observed variations in air exchange rates for the ASU House and Indianapolis House, compared with EPA's summary of the distribution of typical residential air exchange rates.[29,30] Examination of these distributions point in a clear direction for modifying the model of VI. Instead of using a constant value of air exchange rate, as is customary, its values should be parameterized. A higher air exchange would of course be associated with lower c_{in} and vice versa. Moreover, A_e may sometimes be correlated with $p_{\text{in/out}}$. Determining any general relationship between A_e and $p_{\text{in/out}}$ is difficult: the structure itself and weather phenomena have a significant effect on air exchange. As the data in the supplementary data show (Figure S1), there is no easily discernable correlation between these variables at the ASU site, though there is a hint of slight seasonal dependence.

To show the influence of possible statistical fluctuations of air exchange rate on the predictions of α_{gw} values, the scenarios of Figure 6 were rerun calculated using the 5th and 95th percentile A_e values, 0.17 and 0.90 respectively (based upon the actual distributions in Figure S1), providing predicted upper and lower bounds for α_{gw}. These bounds are given by the shaded blue regions around the center line calculated for an assumed constant A_e of 0.5 per hour.

It is apparent that assuming variability in air exchange rate allows capturing most of the observed variability in α_{gw}. We believe that this explains the portion of the variation in indoor air contaminant concentration data that cannot be explained by either existence of preferential pathways or by the range in indoor depressurization. Thus we believe that it is the interplay of preferential pathway conditions, with indoor pressure variations and normal

air exchange rates that help to explain the observations of significant variations in reported indoor air contaminant concentrations.

Results of Transient Simulations

Figure 7: Transient simulation of a "typical" VI day, using diurnal indoor/outdoor pressure difference and air exchange rate as inputs. Effect of preferential pathway considered.

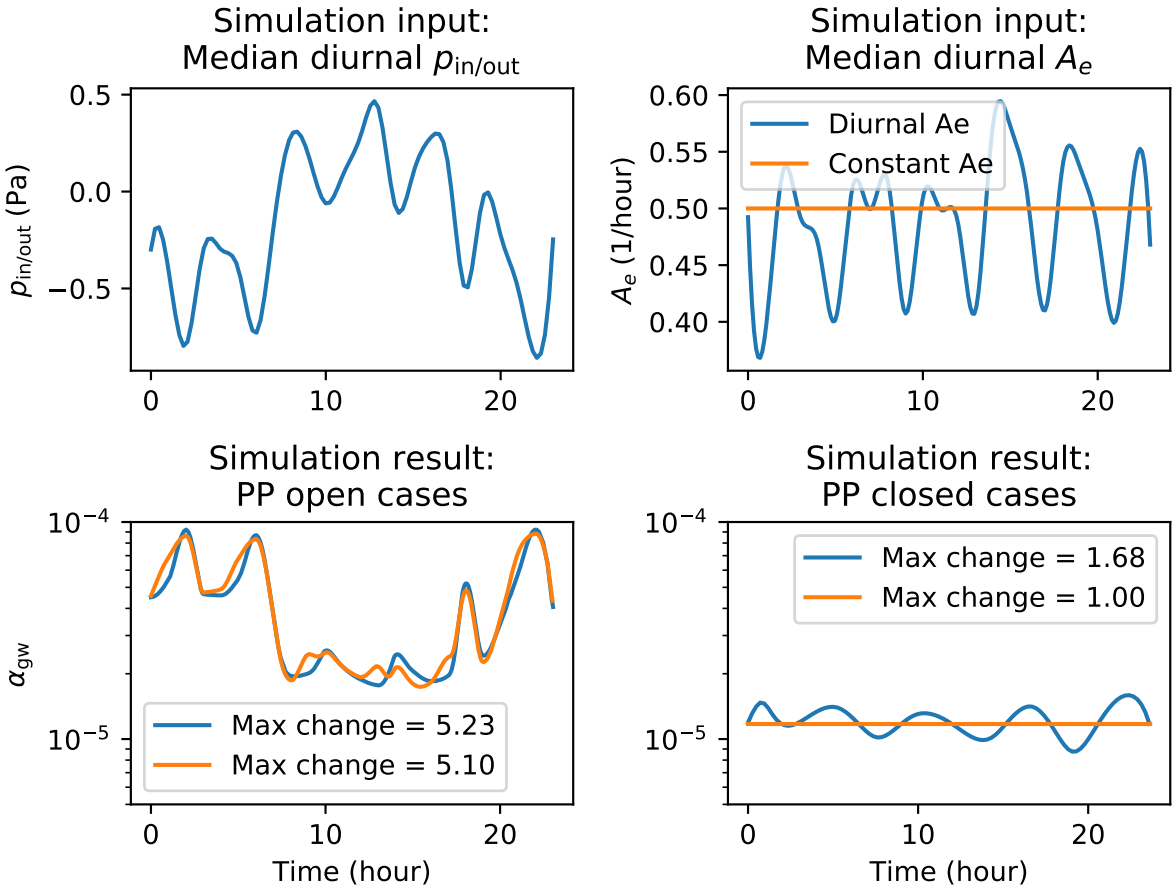

The above analyses have been conducted under simulated steady state conditions. The final test of the conclusions reached above comes in applying them in an actual transient simulations. We run the model described in Figure 2 and run 24-hour simulations to see how c_{in} fluctuates over a "typical" day, and how much of these fluctuations are attributed to air exchange rate versus indoor/outdoor pressure difference. This is achieved by using varying $p_{in/out}$ as one model input, and then running a scenario where A_e also fluctuates, and one

where A_e is constant throughout the entire simulation period. Just like before, we consider this effect for both the preferential pathway open and closed cases.

Using the ASU House dataset, the "typical" daily $p_{\text{in/out}}$ is found by querying the data what the median, hourly, diurnal $p_{\text{in/out}}$ was during the non-CPM periods, giving us the median $p_{\text{in/out}}$ at 00:00, ..., 13:00, ..., 23:00. This "typical" $p_{\text{in/out}}$ cycle may be seen in the upper left panel of Figure 7 (note that values between the hourly medians are interpolated using cubic splines). The "typical" air exchange rate is calculated in exactly the same way and is shown by the blue line in the upper right panel of Figure 7. The orange line is the constant air exchange rate value used.

The result of these simulations may be seen in the bottom two panels of Figure 7, where the left and right panels show the preferential pathway open and closed respectively scenarios. The "max change" value in the legends is the quotient between the lowest and highest concentrations, i.e. a value of two indicate that the maximum daily concentration is twice as high as the lowest. This is the same property that is plotted in Figure 3.

When the preferential pathway is open, we see that there is a maximum change of a factor by around 5, irrespective if A_e fluctuates or not, which is somewhat more than the maximum daily variation shown in Figure 3. The relatively small difference between the diurnal and constant A_e cases indicate that most of the variability during a "typical" day is here attributable to fluctuations in $p_{\text{in/out}}$. This is to be expected as we have already established that the preferential pathway increased the "advective potential", i.e. increasing the influence of $p_{\text{in/out}}$ on contaminant entry rate. Even for the small fluctuations in $p_{\text{in/out}}$, under the influence of this type of preferential pathway, the contaminant entry rate is a more significant than the contaminant exit rate, which determined by air exchange rate.

When the preferential pathway is closed the story is quite different. Here we see that when air exchange rate is held constant, there is essentially no variation in c_{in}. This is again not surprising, as Figure 6 demonstrate that when the preferential pathway is closed, the influence of $p_{\text{in/out}}$ on contaminant entry rate (and subsequently c_{in}) is small (which is further

compounded by the small changes in $p_{\text{in/out}}$). When the air exchange rate is fluctuating the maximum change in c_{in} is 1.68, which is in line with what is shown in Figure 3, showing that for a "typical" day, much of the daily variation in c_{in} is due to daily fluctuations in air exchange rate.

All of this show the complicated nature of temporal variability in c_{in}. It is important to remember that we have only considered the effect of indoor/outdoor pressure difference and air exchange rate in this artcile, but slower processes, e.g. changes in groundwater contaminant concentration or various seasonal effects has a significant impact on VI over time, which we will address in future articles, are too of importance. But for shorter time periods, temporal variability in indoor contaminant concentration is dominated by indoor/outdoor pressure difference and/or air exchange rate.

For a site where the communication between the subsurface and the indoor is good i.e. advective transport is significant, $p_{\text{in/out}}$ is or may be the most significant determinant of c_{in} and its temporal variability. In this paper we show that that such a scenario may arise due to a preferential pathway, such as the one at the ASU House. But these conditions may also exist even in the absence of a preferential pathway as the NAS North Island demonstrate. At sites where advective transport is not as significant much of the (especially shorter-term) temporal variability in c_{in} may be attributed to fluctuations in air exchange rate.

Acknowledgement

This project was supported by grant ES-201502 from the Strategic Environmental Research and Development Program and Environmental Security Technology Certification Program (SERDP-ESTCP).

References

(1) U.S. Environmental Protection Agency, OSWER Technical Guide for Assessing and

Table 4: List of abbreviations

A_{ck}	Crack area
A_e	Air exchange rate
$\alpha,\ n,\ m,\ l$	van Genuchten parameters
α_{gw}	Attenuation from groundwater contaminant vapor source
c_{in}	Indoor air contaminant concentration
c	Soil-gas contaminant concentration
c_w	Soil-water contaminant concentration
c_{gw}	Contaminant groundwater concentration
χ	Preferential pathway contaminant concentration scaling parameter
D_{eff}	Effective diffusion coefficient
D_{air}	Diffusion coefficient in air
D_{water}	Diffusion coefficient in water
j_{ck}	Contaminant molar flux through the foundation crack
κ_s	Saturated soil permeability
K_H	Dimensionless Henry's law constant
k_r	Relative permeability
L_{slab}	Thickness of the foundation slab
M	Molar mass
μ	Contaminant vapor viscosity
NAS	Naval Air Stations
p	Pressure in soil
$p_{\text{in/out}}$	Indoor/outdoor pressure difference
PP	Preferential pathway
ρ	Density
Se	Soil water saturation
t	time
θ_g	Vapor/gas filled porosity
θ_w	Water filled porosity
θ_r	Residual water filled porosity
θ_t	Total porosity
$\vec{u}$	Soil-gas velocity (vector quantity)
VI	Vapor intrusion
V_{base}	Basement volume
z	Elevation above groundwater

Mitigating the Vapor Intrusion Pathway From Subsurface Vapor Sources To Indoor Air.

(2) Folkes, D.; Wertz, W.; Kurtz, J.; Kuehster, T. Observed Spatial and Temporal Distributions of CVOCs at Colorado and New York Vapor Intrusion Sites. *29*, 70–80.

(3) Holton, C.; Luo, H.; Dahlen, P.; Gorder, K.; Dettenmaier, E.; Johnson, P. C. Temporal Variability of Indoor Air Concentrations under Natural Conditions in a House Overlying a Dilute Chlorinated Solvent Groundwater Plume. *47*, 13347–13354.

(4) Johnston, J. E.; Gibson, J. M. Spatiotemporal Variability of Tetrachloroethylene in Residential Indoor Air Due to Vapor Intrusion: A Longitudinal, Community-Based Study. *24*, 564.

(5) Hosangadi, V.; Shaver, B.; Hartman, B.; Pound, M.; Kram, M. L.; Frescura, C. High-Frequency Continuous Monitoring to Track Vapor Intrusion Resulting From Naturally Occurring Pressure Dynamics. *27*, 9–25.

(6) McHugh, T.; Loll, P.; Eklund, B. Recent Advances in Vapor Intrusion Site Investigations. *204*, 783–792.

(7) U.S. Environmental Protection Agency, Assessment of Mitigation Systems on Vapor Intrusion: Temporal Trends, Attenuation Factors, and Contaminant Migration Routes under Mitigated And Non-Mitigated Conditions.

(8) Johnson, P. C.; Holton, C. W.; Guo, Y.; Dahlen, P.; Luo, E. H.; Gorder, K.; Dettenmaier, E.; Hinchee, R. E. Integrated Field-Scale, Lab-Scale, and Modeling Studies for Improving Our Ability to Assess the Groundwater to Indoor Air Pathway at Chlorinated Solvent-Impacted Groundwater Sites.

(9) Holton, C. W. Evaluation of Vapor Intrusion Pathway Assessment Through Long-Term Monitoring Studies.

(10) Guo, Y. Vapor Intrusion at a Site with an Alternative Pathway and a Fluctuating Groundwater Table.

(11) Guo, Y.; Holton, C.; Luo, H.; Dahlen, P.; Gorder, K.; Dettenmaier, E.; Johnson, P. C.

Identification of Alternative Vapor Intrusion Pathways Using Controlled Pressure Testing, Soil Gas Monitoring, and Screening Model Calculations. *49*, 13472–13482.

(12) McHugh, T.; Beckley, L.; Sullivan, T.; Lutes, C.; Truesdale, R.; Uppencamp, R.; Cosky, B.; Zimmerman, J.; Schumacher, B. Evidence of a Sewer Vapor Transport Pathway at the USEPA Vapor Intrusion Research Duplex. *598*, 772–779.

(13) Pennell, K. G.; Scammell, M. K.; McClean, M. D.; Ames, J.; Weldon, B.; Friguglietti, L.; Suuberg, E. M.; Shen, R.; Indeglia, P. A.; Heiger-Bernays, W. J. Sewer Gas: An Indoor Air Source of PCE to Consider During Vapor Intrusion Investigations. *33*, 119–126.

(14) Roghani, M.; Jacobs, O. P.; Miller, A.; Willett, E. J.; Jacobs, J. A.; Viteri, C. R.; Shirazi, E.; Pennell, K. G. Occurrence of Chlorinated Volatile Organic Compounds (VOCs) in a Sanitary Sewer System: Implications for Assessing Vapor Intrusion Alternative Pathways. *616-617*, 1149–1162.

(15) Riis, C. E.; Christensen, A. G.; Hansen, M. H.; Husum, H.; Terkelsen, M. Vapor Intrusion through Sewer Systems: Migration Pathways of Chlorinated Solvents from Groundwater to Indoor Air. Seventh International Conference on Remediation of Chlorinated and Recalcitrant Compounds.

(16) Nielsen, K. B.; Hvidberg, B. Remediation Techniques for Mitigating Vapor Intrusion from Sewer Systems to Indoor Air. *27*, 67–73.

(17) Brenner, D. Results of a Long-Term Study of Vapor Intrusion at Four Large Buildings at the NASA Ames Research Center. *60*, 747–758.

(18) McHugh, T. E.; Beckley, L.; Bailey, D.; Gorder, K.; Dettenmaier, E.; Rivera-Duarte, I.; Brock, S.; MacGregor, I. C. Evaluation of Vapor Intrusion Using Controlled Building Pressure. *46*, 4792–4799.

(19) Jones, E.; Oliphant, T.; Pearu Peterson, SciPy: Open Source Scientific Tools for Python.

(20) Shen, R.; Pennell, K. G.; Suuberg, E. M. Influence of Soil Moisture on Soil Gas Vapor Concentration for Vapor Intrusion. *30*, 628–637.

(21) Yao, Y.; Wang, Y.; Zhong, Z.; Tang, M.; Suuberg, E. M. Investigating the Role of Soil Texture in Vapor Intrusion from Groundwater Sources. *46*, 776–784.

(22) Yao, Y.; Mao, F.; Ma, S.; Yao, Y.; Suuberg, E. M.; Tang, X. Three-Dimensional Simulation of Land Drains as a Preferential Pathway for Vapor Intrusion into Buildings. *46*, 1424–1433.

(23) Richards, L. A. Capillary Conduction of Liquids through Porous Mediums. *1*, 318–333.

(24) van Genuchten, M. T. A Closed-Form Equation for Predicting the Hydraulic Conductivity of Unsaturated Soils. *44*, 892–898.

(25) Millington, R. J.; Quirk, J. P. Permeability of Porous Solids. *57*, 1200.

(26) Dan, H.-C.; Xin, P.; Li, L.; Li, L.; Lockington, D. Capillary Effect on Flow in the Drainage Layer of Highway Pavement. *39*, 654–666.

(27) Abreu, L. D. V.; Schuver, H. Conceptual Model Scenarios for the Vapor Intrusion Pathway.

(28) U.S. Environmental Protection Agency, Users's Guide For Evaluating Subsurface Vapor Intrusion Into Buildings.

(29) U.S. EPA, Exposure Factors Handbook 2011 Edition.

(30) M. D. Koontz,; H. E. Rector, Estimation of Distributions for Residential Air Exchange Rates.